Photorefractive moiré-like patterns with different variation directions for multi-projection in profilometer applications.

G.N.Oliveira[a], M.E. de Oliveira[b], J.Dias.[b], and P.A.M. dos Santos*[b]

[a] Laboratório de Mecânica Teórica e Aplicada, Departamento de Engenharia Mecânica, Universidade Federal Fluminense, Rua Passo Pátria, 156, Niterói, R. J., Brazil, Cep.: 24.210-240; [b] Instituto de Física, Laboratório de Óptica Não-linear e Aplicada, Universidade Federal Fluminense, Av. Gal. Nilton Tavares de Souza, s/n, Gragoatá, Niterói, R. J., Brazil, Cep.: 24.210-346.

ABSTRACT

In the present paper we describe the holographic interferometric beating to produce dynamic photorefractive moiré-like patterns with two or more variation directions. It has been experimentally obtained by the superposition of two sinusoidal gratings with slightly different pitches for each direction of fringe variation obtained. These dynamic moiré-like patterns are induced in the volume of the $Bi_{12}TiO_{20}$ (BTO) crystal sample used as dynamic holographic medium. The Fourier transform profilometry method is applied using two or more moiré fringe patterns with different direction of variations, simultaneously or not, projected onto an object surface.

Keywords: moiré, digital holography, Fourier, optical beating

1. INTRODUCTION

Usually one direction variation moiré-like interferometric pattern is produced when any two regular periodic superimposed structures are illuminated. For example, the superposition of two Ronchi rulers with slightly different superimposed pitches, produces one direction regularly spaced light fringes that have been used in many optical applications. Such moiré-like patterns have been traditionally employed in profilometry and optical metrology[1], as non-destructive testing in mechanical engineering, medical sciences, material science and so, covering a lot of many different kinds of studies and applications.

In the present work we describe the holographic interferometric beating to produce dynamic photorefractive moiré-like patterns with two or more variation directions. It has been experimentally obtained by the superposition of two sinusoidal gratings with slightly different pitches for each direction of fringe variation obtained. These dynamic moiré-like patterns are induced in the volume of the $Bi_{12}TiO_{20}$ (BTO) crystal sample used as dynamic holographic medium.

Basically, the dynamic photorefractive moiré-like patterns with low spatial frequencies, are used for profile determination of small objects. The Fourier transform profilometry method is applied using two or more moiré fringe patterns with different direction of variations, simultaneously or not, projected onto an object surface. We show that the use of this kind of procedure has some important advantages comparatively to the use only one interferometric pattern projection in Fourier transform profilometry, mainly in the capacity to overcome the intrinsic difficulties related to topographic inhomogeneity, irregularities and discontinuities problems in some objects of interest.

2. DYNAMIC MOIRÉ-LIKE PATTERNS FOR MULTI-PROJECTION

In this section the dynamic moiré-like patterns are described as originated by the interaction of two sinusoidal high frequency gratings holographically generated, both induced in the volume of the photorefractive crystal sample, the dynamic holographic media. In the photorefractive effect, one dynamic holographic sinusoidal phase grating could be obtained after illuminating the BTO sample by the interference pattern given by

$$I(x) = I_o\left(1 + M\cos k_g x\right) \tag{1}$$

In eq.(1) $k_g = 2\pi/\Lambda$ (where Λ is the grating spacing) is the grating wave number and M is the fringe modulation rate in the projected interference pattern.

8th Iberoamerican Optics Meeting and 11th Latin American Meeting on Optics, Lasers, and Applications, edited by Manuel Filipe P. C. Martins Costa, Proc. of SPIE Vol. 8785, 878556

After illuminating the sample, taking into account the band transport model [8], the photogenerated carrier displacements, with subsequent trapping, produce a volume space charge electric field given by [9]

$$E_{SC}(x) = \frac{Dk}{\mu}\frac{m\sin(kx)}{1+m\cos(kx)} \tag{2}$$

where D is the diffusion constant, μ is the mobility and the parameter m is the induced modulation rate. Then, due to the linear electro-optic effect exhibited by the photorefractive materials, a spatial refractive index modulation is produced. This spatial refractive index modulation is given by

$$\Delta n(x) = \frac{1}{2} r_{41} n_0^3 E_{SC}(x) = \Delta n_0 \sin(k_g x) \tag{3}$$

and the diffraction efficiency is

$$\eta = \left[\frac{\pi \Delta n(x)}{\lambda \cos(\theta_B)} m \frac{\sin(\rho l)}{\rho}\right]^2 \tag{4}$$

where θ_B is the incident Bragg angle, λ is the laser light source wavelength, ρ is the optical activity parameter and l is the crystal sample thickness. After superposition of two sinusoidal phase gratings of different spacing in the sample volume, two index modulations, $\Delta n_1(x)$ and $\Delta n_2(x)$, both defined by Eq. (3), with slightly different spatial frequencies k_{g1} and k_{g2}, are produced. Then the refraction index modulation resulting of this superposition is [10]

$$\Delta n(x) = 2\Delta n_0 \cos(k_g^m x)\sin(\bar{k}_g x) \tag{5}$$

where $\bar{k}_g = (k_{g1} + k_{g2})/2$ is the average spatial frequency and $k_g^m = (k_{g1} - k_{g2})/2$ is the modulation spatial frequency.

The spatial frequencies, k_{g1} and k_{g2}, have high values and, in addition, their values are comparable, that is, $k_{g1} \sim k_{g2}$; in this case, $\bar{k}_g >> k_g^m$ and the resulting photorefractive index modulation in the sample volume is spatially modulated. This means that a moiré-like fringe pattern is produced like a beat phenomenon, due to the dynamic superposition of two sinusoidal phase gratings in the BTO crystal sample volume.

3. FOURIER TRANSFORM PROFILOMETRY

In the present work the dynamic moiré-like pattern produced by photorefraction, is the projected interference fringe pattern onto an object surface. Then, using the Fourier transform method [3,4], the object profile could be precisely determined. In this method only one image of the fringe pattern projection is necessary. Therefore, it is simple and efficient. The produced and projected fringe pattern can be represented by the amplitude[5]

$$g(x,y) = a(x,y) + b(x,y)\cos[2\pi\nu_0 x + \phi(x,y)] \tag{6}$$

where the phase $\phi(x,y)$ contains information about the object. The amplitudes $a(x,y)$ and $b(x,y)$ are the irradiance variations produced by the object.

The essence of the proposed method consists of extracting $\phi(x,y)$ from Eq. (6) that is rewritten in the following form:

$$g(x,y) = a(x,y) + c(x,y)\exp(2\pi\nu_0 x) + c^*(x,y)\exp(-2\pi\nu_0 x) \tag{7}$$

where

$$c(x,y) = \frac{1}{2} b(x,y)\exp[i\phi(x,y)] \tag{8}$$

that is easily obtained by rewriting Eq. (6) using exponentials, and * means complex conjugate.

The next step is to obtain the Fourier transform of Eq. (7) with respect to *x,* that is the Fourier spectra

$$G(\nu,y) = A(\nu,y) + C(\nu-\nu_0,y) + C^*(\nu-\nu_0,y) \tag{9}$$

where ν is the spatial frequency in the *x* direction.

Due to the fact that *a(x,y), b(x,y)* and the phase $\phi(x,y)$ have very slow spatial variations with respect to the spatial frequency ν_0, the Fourier spectrum in Eq. (9) has two displaced components by the carrier frequency ν_0 , as shown in Fig.1. This means that lateral function $C(\nu-\nu_0,y)$ or $C^*(\nu-\nu_0,y)$ could be translated to spectrum origin (see down in Fig. 1); after filtering the background $A(\nu,y)$, the Fourier transform of $C(\nu,y)$, for example, with respect to ν_0 , will give $c(x,y)$ defined by Eq. (5), where the phase map $\phi(x,y)$ can be determined by a convenient unwrapping process[6].

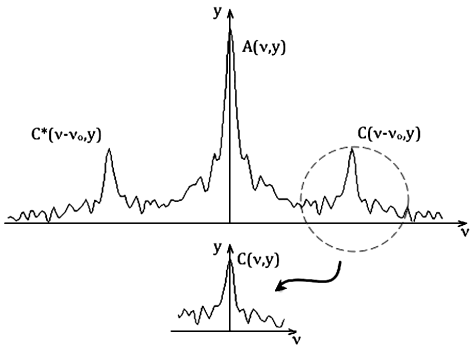

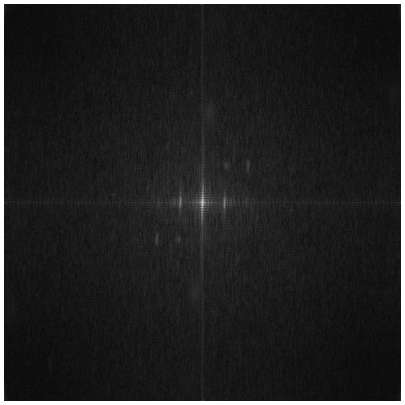

Fig. 1. Fourier spectrum of Eq. (7) showing the component $C(\nu-\nu_0,y)$ displaced to the origin In the right side of this figure is the experimental unidirectional Fourier spectrum

4. EXPERIMENTAL SETUP

The photorefractive holographic setup has been used in anisotropic two wave mixing architecture [7,8], in diffusion only recording mechanism[9]. This means that the observed moiré-like fringe patterns, with low spatial frequencies (~2-5 lines mm^{-1}), are produced like a beat phenomenon [10], due to the dynamic superposition of two sinusoidal phase gratings in the BTO crystal sample volume.

The experimental holographic setup, indicated in Fig. 2, shows two beams with λ= 0.633μm coming to a He-Ne laser light source with 35mw nominal power. BS is a variable beam splitter; C's are collimators and M1, M2, M3, M4 and M5 are mirrors.

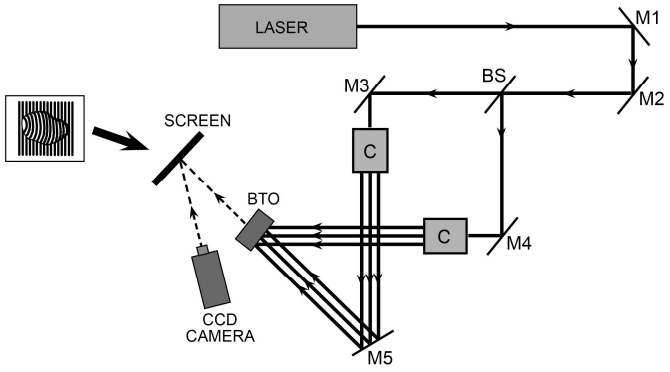

Fig. 2. Experimental holographic setup

The laser light beams, one being the "object" beam and another the reference beam are projected on the BTO crystal (8x8x8 mm^3) entrance face at an angle $\theta_B \sim 23^0$. This means, according to the classic Bragg's law, that a sinusoidal phase grating with 1,000 lines mm^{-1} of spatial frequency is produced. At this moment one shutter (not shown in the figure) covering both beams is closed, and mirror M5 is rotated by $\sim 1^0$. In this way, by opening the shutter, an additional sinusoidal phase grating is produced with a small difference in the spatial frequency. Reading both gratings by the beam from mirror M4, the moiré-like pattern is produced and projected on the screen, where the object is placed. The object is a half of small polished metallic cylinder with 1.90 mm of radius and 25 mm of length, fixed on an also polished metallic plate (50x70 mm^2). The moiré-like pattern produced after the interaction of two sinusoidal phase gratings and projected onto the sample, to determine its profile, is indicated in Fig. 3. These images are captured by a CCD camera interfaced to a computer.

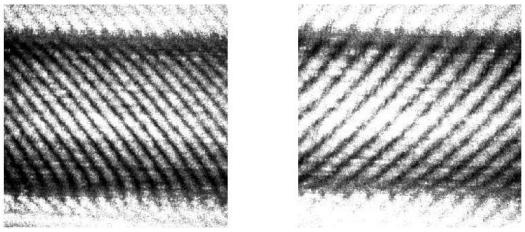

Fig. 3. Two different dynamic moiré-like fringe patterns projected onto the object surface, a small cylinder. In both images are shown one-dimensional moiré pattern projected with 45 (right) and 135 (left) degrees of inclination each one from the horizontal direction.

5. RESULTS AND DISCUSSION

In order to produce the digital holographic moiré patterns, the M3 mirror rotation is carefully controlled by a step motor connected to a computer. After experimental procedures previously described we obtained the fringe patterns projected onto the test object. The first one is the image shown in **Fig.3**, resulting from the dynamic fringe pattern produced by the holographic setup. The second one, in **Fig. 4**, is the 2D dynamic moiré-like fringe pattern projected onto the object surface, a small cylinder. This pattern could be obtained by the superposition of the two moiré patterns indicated in Fig.3 in sequence onto the surface of the object.

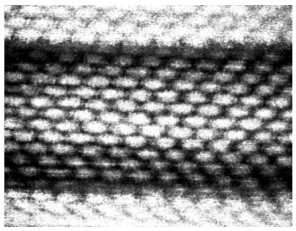

Fig. 4. 2D dynamic moiré-like fringe pattern projected onto the object surface, a small cylinder. In this image are shown the obtained moiré pattern produce with the superposition of the two patterns of the Fig.3 simultaneously, holographically produced in sequence.

In order to find the object profile the steps proposed in the section 3 must be performed. Through a single image of a fringe pattern of **Fig.4**, resulting from the both patterns of Fig.3 simultaneously projected onto the object surface, the Fourier transform is obtained (see **Fig. 5**). These steps were performed using the public domain *Idea* software [11] and analyzed by the public domain *NIH Image* software [12]

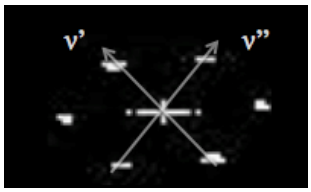

Fig. 5. Fourier spectrum of the moiré pattern projected over the object in **Fig.4.**

Observe that due to 2D pattern we have two component *C* that could be displaced to the origin from two original positions using two directions ν' and ν'' , that is, the two main variation directions of the fringes in the **Fig 3**. The next step is the production of the phase map (not shown) that will be wrapped. Using the same public domain *Idea* software [11] unwrapping operation is realized and finally the 3D-profile is obtained(see Fig.6)

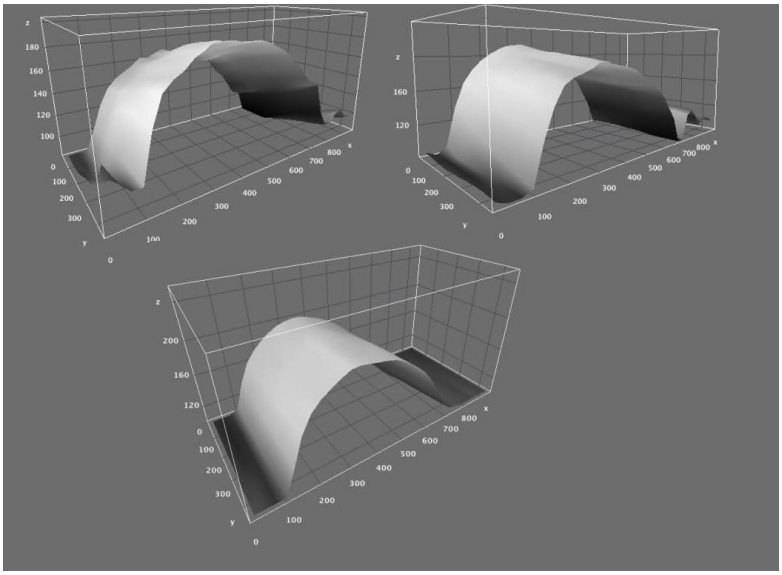

Fig. 6. Uncalibrated optical 3D profile of object after phase unwrapping from dynamic moiré fringe pattern projection illustrated in the Fig.4. It was obtained using the components C displaced from the spectrum illustrated in **Fig.5**

Its quite clear by the results presented in Fig.6. that the 3D profiles calculated using the Fourier method for each fringe projection with frequencies ν' and ν'' individually (two profiles up in Fig.6) have many topological defects and some distortions. On the other hand, by using the both patterns to compose a multi-projection in the Fig.4, that is, adding the information given by ν' and ν'' front the resulting spectrum of Fig.5 there is a considerable improvement in the 3D profile obtained (the profile down in the Fig.6) eliminating the most of limitations presented using the single projections.

6. CONCLUSION

In the present paper we have demonstrated, as far as we know, at first time that the Fourier transform profilometry method is applied using two or more moiré fringe patterns with different direction of variations, simultaneously or not, projected onto an object surface. We show that the use of this kind of procedure has some important advantages comparatively to the use only one moiré-like fringe pattern projection in Fourier transform profilometry. Mainly in the capacity to overcome the intrinsic difficulties related to topographic inhomogeneity, irregularities and discontinuities problems in some objects of interest.

It is clear by these observations that the dynamic moiré-like fringe patterns, from the above described experimental conditions, can be used to determine the optical 3D profiles with some advantages, comparatively to the results obtained by the classical unidirectional fringe projection methods. Best 2D fringe pattern contrast, less speckle noise, absence of noises produced by spurious reflections and a pure sinusoidal shape from the holographic moiré-like process are some advantages of the dynamic moiré-like pattern in the proposed analysis

Acknowledgements. We would like to thank to Dr. I. Costa for the great help in text spelling and grammar corrections, and to the Brazilian financial support agencies CNPq (Conselho Nacional de Pesquisa), CAPES (Coordenadoria de Aperfeiçoamento de Pessoal de Nível Superior) and FAPERJ (Fundação Carlos Chagas Filho de Apoio a Pesquisa do Estado do Rio de Janeiro

REFERENCES

[1] Huang, L., Kemao, Q., Pan, B. and Asundi, A.K., "Comparison of Fourier transform, windowed Fourier transform, and wavelet transform methods for phase extraction from a single fringe pattern in fringe projection profilometry," Opt. Las. Eng. 48, 141 (2010).

[2] Takasaki, H., "Moiré Topography," App. Opt. 12, 845 (1973).

[3] Takeda, M., Ina, H. and Kobayashi, S., "Fourier-transform method of fringe-pattern analysis for computer-based topography and interferometry," J. Opt. Soc. Am. 72, 156 (1982).

[4] Takeda, M. and Mutoh, K., "Fourier transform profilometry for the automatic measurement of 3-D object shapes," Appl. Opt. 22, 3977 (1983).

[5] Su, X., Zhou, W., von Bally, G. and Vukicevic, D., "Automated phase- measuring profilometry using defocused projection of the Rochi grating," Opt. Comm. 94, 561 (1992).

[6] Quan, C., He, X.Y., Wang, C.F., Tay, C.J. and Shang, H.M., "Shape measurement of small objects using LCD fringe projection and phase shifting," Opt. Comm. 189, 21 (2001).

[7] Kukhtarev, N.V., Markov, V.B., Odulov, S.G., Soskin, M.S. and Vinetskii, V.L., "Holographic storage in eletrooptic crystals: 2 beam coupling - light amplification," Ferroelectrics 22, 949 (1979).

[8] Yeh, P., "Introduction of Photorefractive Nonlinear Optics," Wiley, (1993).

[9] dos Santos, P.A.M. and de Oliveira, G.N., "Holographic Fourier synthesis of dynamic moiré-like patterns in the photorefractive $Bi^{12}TiO^{20}$," Opt. Eng. 44, 12 (2005).

[10] dos Santos, P.A.M., "Moiré-like patterns as a spatial beat frequency in photorefractive sinusoidal phase gratings superposition," Opt. Comm. 212, 211 (2002).

[11] See the website at http://optics.tu-graz.ac.at.

[12] See the website at http://rsbweb.nih.gov/ij.

[13] Martínez, A., Rayas, J.A., Cordero, R. and Genovese, K., "Analysis of optical configurations for ESPI," Opt. Laser Eng. 46, 48 (2008).

[14] Martínez, A., Rayas, J.A., Flores, J.M., Vera, R.R. and Aguayo, D.D., "Técnicas ópticas para el contorneo de superficies tridimensionales," Rev. Mex. Fis. 431, 51 (2005).

*Corresponding author: pams@if.uff.br